Genetic Algorithm Tuned Super Twisted Sliding Mode Controller (STSMC) for Self-balancing Control of a Two-Wheel Electric Scooter

Tefera T. Yetayew[1(✉)] and Daniel G. Tesfaye[2]

[1] Adama Science and Technology University, P.O. 1888, Adama, Ethiopia
[2] Wolayta Sodo University, Sodo, Ethiopia

Abstract. Two wheel self-balancing electric scooter is based on inverted pendulum system and this system is a nonlinear and unstable. An inertial measurement unit (IMU) which is combination of accelerometer and gyroscope measurement is used in order to estimate and obtain the tilt angle of the scooter. Super twisted sliding mode controller (STSMC) is applied to correct the error between the desired set point and the actual tilt angle and adjust the brushless direct current (BLDC) motor speed accordingly to balance the scooter, when scooter is tilted forward, motor is move forward to catch up in order to balance the scooter and proportional integral derivative (PID) controller is used to control direction of scooter that means to turn left or right. The STSMC parameters and PID parameters are tuned using genetic algorithm (GA) and controllers performance evaluation is done using MATLAB/Simulink. The pitch and yaw angle with changes in magnitude of 0.1 rad and zero reference angle, almost the steady state error are 7.965×10^{-08} and 5.677×10^{-07} respectively for both controllers tuned by GA. GA tuned controllers are compared with analytically tuned controlled for initial pitch angle of 0.3 rad. The magnitude of steady-state errors at time 2 s are 7.71×10^{-07} and 0.004648 respectively, which is an indication of parameters tuned using global optimization algorithms, in this case GA are more optimal than analytically tuned parameters.

Keywords: Scooter · Genetic algorithm · STSMC and PID controller

1 Introduction

In today's society transportation is undoubtedly a fast-growing industry. Due to the rapid growth in the demand for personal transporter vehicles, self-balancing personal transporter scooters were introduced by the Segway Company. For the intention of increasing the efficiency of human's transportation and to reduce the cost, the self-balancing personal transporter which is also a great representation of the personal mobility device concept is now widely used in many industries and institutions such as police departments, tourism industry, factories and so on. The benefits which are offered by this personal transporter vehicle such as higher accessibility and zero fuel consumption can be considered as the ultimate solutions for the upcoming global issues

M. L. Berihun (Ed.): ICAST 2021, LNICST 411, pp. 269–287, 2022.
https://doi.org/10.1007/978-3-030-93709-6_18

caused by the growth of traffic and the environmental pollution happening all around the world. Even though the self-balancing transporter represents a better version of the personal transporter type vehicles that are being used nowadays, it simply failed in reaching the hands of the majority of society due to the expensive price range and the safety issues pointed out by the existing users of these self-balancing transporter models [1, 2].

The self-balancing personal transporter models (mainly Segway models) are comprised of multiple gyroscope and accelerometer sensors (few as additional) to obtain the angular rate and acceleration readings along different axes. The drawback which comes along using multiple sensors is the additional cost and the extra computational power required by the control unit. The two-wheeled self-balancing robot is a nonlinear MIMO under actuated system; thus, it is very challenging to keep balance when it climbs or descends on a slope and, especially, in the presence of no measurable disturbances. Two-wheeled scooters are one of the modern research topics in the robotic fields due to the natural unstable dynamic systems around the world [2–5]. Two-wheeled self-balancing robot based on inverted pendulum theory and dynamic balancing systems.

The contents of the research organizes the basics lay-out, components and principles in section two of the research and the dynamic models of the self-balance scooter in section three. The controllers design, tuning both analytically and GA based is presented in section four of the research. The results with the corresponding discussions and concluding remarks of findings are presented in sections five and six of the research.

2 Two-Wheel Self-balancing Scooter Basics

The research in recent years reveals the idea of self-balancing scooters. The two wheel self-balancing scooter is represented schematically in Fig. 1. Once system balance is achieved the system can move forward and back ward directions [6, 7].

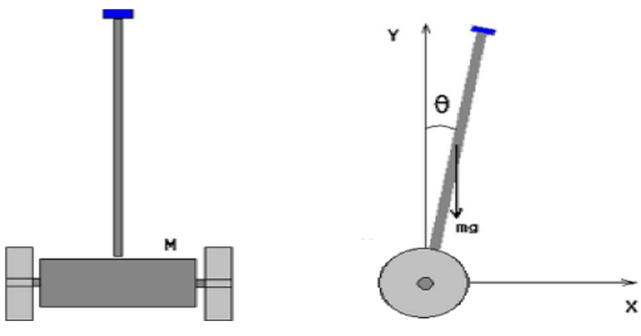

Fig. 1. Side and front views of the ideal two wheeled inverted pendulum system [6]

The pendulum that may cause system instability, the main body of the scooter that carries the drive system and the wheels for forward and backward movement are the main components of the two wheel self-balancing scooter considered in this research [6–8].

In principle, the controller for the self-balancing two wheel scooter, reads the tilt and compensates for the error so that the required upright position of the system will be kept. And also should respond to external forces as disturbance to the normal motion of the scooter by which the required position of the scooter can be maintained [7, 8] (Fig. 2).

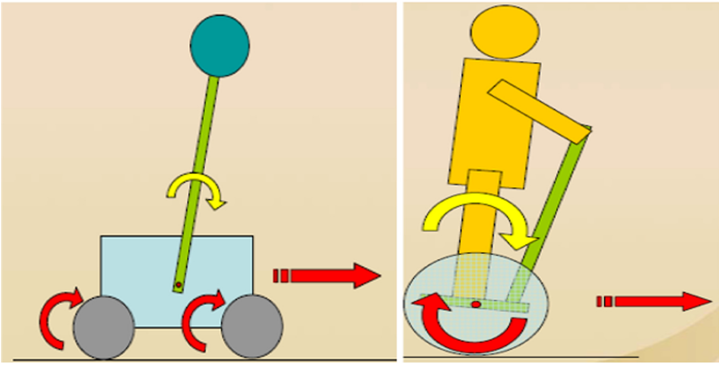

Fig. 2. Working principle of scooter [8]

3 Mathematical Model of the System

3.1 Mathematical Model of Scooter

To design the controller and perform the required analysis, the electrical actuator and the mechanical system of the scooter needs to be represented mathematically. Table 1 gives the required parameters of the scooter.

Table 1. Parameter and descriptions of scooter [8–10].

Parameters	Description	Unit
T_L and T_R	Input torque of the left and right wheel	N.m
H_{TR} and H_{TL}	Friction between the ground and the right and left wheels	N
H_R and H_L	Reaction forces impact on the right and left wheels	N
J_{TL} and J_{TR}	Inertial moment of the rotating masses with respect to the z axis	N.m
θ_{WR} and θ_{WL}	Pitch angle of the right and left wheels	rad
J_B	Inertial moment of the chassis with respect to the z axis	N m

The mathematical model of scooter is separated into 3 parts.

1. Wheel
2. Body
3. Dc motor (actuator)

In order to determine mathematical model of the electric scooter newton method is applied (Fig. 3).

Fig. 3. Force analysis of right and left-wheel [8]

For the left wheel of the eScooter (the same as the right wheel):
Using Newton's Law of motion on the horizontal axis X

$$\sum F_x = ma$$

$$M_W \ddot{x}_{WL} = H_{TL} - H_L \tag{1}$$

Using Newton's Law of motion on the vertical axis Y

$$\sum F_Y = ma$$

$$M_W \ddot{y}_{WL} = V_{TL} - V_L - M_W g \tag{2}$$

And the sum of the Moments around the wheel's center gives:

$$\sum M_O = I\alpha$$

$$J_{WL} \ddot{\theta}_{WL} = T_L - H_{TL} R \tag{3}$$

By transforming any linear motion component to an angular motion component by using

$$x_{WL} = \theta_{WL} R \tag{4}$$

Moment of inertia of left wheel

$$J_{WL} = \frac{1}{2} M_{WL} R^2 \tag{5}$$

And for the rotation

$$\delta = \frac{x_{WL} - x_{WL}}{D} \tag{6}$$

From (1) sum the left and right wheel equation

$$\begin{array}{l} + \begin{cases} M_W \ddot{x}_{WL} = H_{TL} - H_L & \text{for the left wheel} \\ M_W x_{WR} = H_{TR} - H_R & \text{for the right wheel} \end{cases} \\ \text{than} \\ M_W(\ddot{x}_{WL} + \ddot{x}_{WR}) = (H_{TL} + H_{TR}) - (H_L + H_R) \end{array} \tag{7}$$

From (3)

$$\begin{cases} J_{WL}\ddot{\theta}_{WL} = T_L - H_{TL}\mathrm{R} & \text{for the left wheel} \\ J_{WR}\ddot{\theta}_{WR} = T_R - H_{TR}\mathrm{R} & \text{for the right wheel} \end{cases} \tag{8}$$

Solve (8) as follow (Fig. 4)

$$\begin{array}{l} H_{TL} = \dfrac{T_L - J_{WL}\theta}{R} \\ H_{TR} = \dfrac{T_R - J_{WR}\theta}{R} \end{array} \tag{9}$$

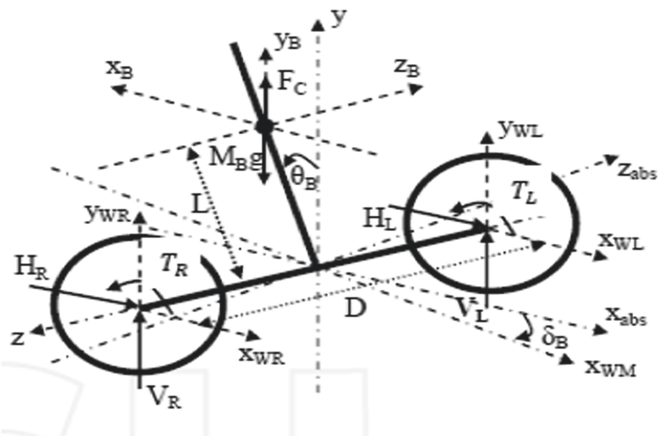

Fig. 4. Coordinate system of body of scooter [8].

For the body of the Scooter:
Using Newton's Law of motion on the horizontal axis X

$$\sum F_x = ma$$

$$M_B \ddot{x}_B = H_L + H_R \tag{10}$$

Using Newton's Law of motion on the vertical axis Y

$$\sum F_y = ma$$

$$M_B \ddot{y}_B = V_L + V_R - M_B g + \frac{T_L + T_R}{L} \sin(\theta_B) \tag{11}$$

The sum of moments around the center of mass of the body

$$\sum M_O = I\alpha$$

$$J_B \ddot{\theta}_B = (V_L + V_R) L \sin(\theta_B) - (H_L + H_R) L \cos(\theta_B) - (T_L + T_R) \tag{12}$$

$$x_B = L \sin(\theta_B) + \frac{x_{WL} + x_{WR}}{2} \tag{13}$$

$$y_B = -L(1 - \cos(\theta_B)) \tag{14}$$

Moment of inertia of chassis

$$J_B = \frac{1}{3} M_B L^2 \tag{15}$$

$$\theta = \theta_B = \theta_W = \theta_{WL} = \theta_{WR} \tag{16}$$

$$x_{WM} = \frac{x_{WL} + x_{WR}}{2} \tag{17}$$

For the chassis rotation:

$$J_\delta \ddot{\delta} = \frac{D}{2} (H_L - H_R) \tag{18}$$

After Solve (8) for $V_L + V_R$ and (7), (13) into (9) than

$$J_B \ddot{\theta} = \left(M_B \ddot{y}_B + M_B g - \frac{T_L + T_R}{L} \sin(\theta) \right) L \sin(\theta) - M_B \ddot{x}_B L \cos(\theta) - (T_L + T_R)$$

$$J_B \ddot{\theta} = M_B L (\ddot{y}_B \sin(\theta) - \ddot{x} \cos(\theta)) + M_B g L \sin(\theta) - (T_L + T_R) \left(1 + \sin^2(\theta)\right) \tag{19}$$

Substitute (14) into (10) than differentiate both side

$$x_B = L\sin(\theta) + x_{WM}$$

$$\dot{x}_B = L\dot{\theta}\cos(\theta) + \dot{x}_{WM}$$

And again differentiate both side

$$\ddot{x}_B = L\ddot{\theta}\cos(\theta) - L\dot{\theta}^2\sin(\theta) + \ddot{x}_{WM} \tag{20}$$

And the same way as x_B differentiate y_B than

$$\ddot{y}_B = -L\ddot{\theta}\sin(\theta) - L\dot{\theta}^2\cos(\theta) \tag{21}$$

Multiply (17) by $\cos(\theta)$ and multiply (18) by $\sin(\theta)$ and subtract both equation than we get

$$\ddot{y}_B\sin(\theta) - \ddot{x}_B\cos(\theta) = -L\ddot{\theta} - \ddot{x}_{WM}\cos(\theta) \tag{22}$$

Substitute (19) and (12) into (16)

$$\frac{4}{3}M_BL^2\ddot{\theta} + M_BL\cos(\theta)\ddot{x}_{WM} = M_BgL\sin(\theta) - (T_L + T_R)\left(1 + \sin^2(\theta)\right) \tag{23}$$

From (10)

$$H_L + H_R = M_B\ddot{x}_B \tag{24}$$

Substitute (9) and (24) into (7)

$$M_W(\ddot{x}_{WL} + \ddot{x}_{WR}) = \left(\frac{T_L + T_R - (J_{WL}\theta + J_{WR}\theta)}{R}\right) - M_B\ddot{x}_B$$

Where $\begin{matrix} J_W = J_{WL} + J_{WR} \\ M_W = M_{WL} + M_{WR} \end{matrix}$ than

$$2M_W\ddot{x}_{WM} = -M_B\ddot{x}_B + \frac{(T_L + T_R)}{R} - \frac{2J_W\ddot{\theta}}{R} \tag{25}$$

From (5)

$$\begin{cases} J_{WL} = \frac{1}{2}M_{WL}R^2 & \text{for left wheel} \\ J_{WR} = \frac{1}{2}M_{WR}R^2 & \text{for right wheel} \end{cases}$$

Sum the two equation

$$\begin{aligned} J_{WL} + J_{WR} &= R^2(M_{WL} + M_{WR}) \\ J_W &= R^2 M_W \end{aligned} \tag{26}$$

Substitute (20) and (26) into (25) than we get

$$(M_B L\cos(\theta) + RM_W)\ddot{\theta} + (2M_W + M_B)\ddot{x}_{WM} = M_B L\dot{\theta}^2\sin(\theta) + \frac{(T_L + T_R)}{R} \tag{27}$$

Solve (23) for $\ddot{x}_{WM}$ and substitute into (27) than

$$\begin{aligned} &\left((2M_W + M_B) - \frac{0.75(M_B L\cos(\theta) + M_W R)\cos(\theta)}{L}\right)\ddot{\theta} = \frac{0.75g(2M_W + M_B)\sin(\theta)}{L} \\ &-0.75M_B\sin(\theta)\cos(\theta)\dot{\theta}^2 - \left(\frac{0.75(2M_W + M_B)\left(1 + \sin^2(\theta)\right)}{M_B L^2} + \frac{0.75\cos(\theta)}{RL}\right)(T_L + T_R) \end{aligned} \tag{28}$$

Solve (23) for $\ddot{\theta}$ and substitute into (27) than

$$\begin{aligned} &\left(-0.75\frac{\cos(\theta)(M_B L\cos(\theta) + M_W R)}{L} + (2M_W + M_B)\right)\ddot{x}_{WM} = -0.75(M_B L\cos(\theta) + M_W R) \\ &\frac{g\sin(\theta)}{L} + M_B L\sin(\theta)\dot{\theta}^2 - \left(0.75\frac{(M_B L\cos(\theta) + M_W R)\left(1 + \sin^2(\theta)\right)}{M_B L^2} + \frac{1}{R}\right)(T_L + T_R) \end{aligned} \tag{29}$$

Solve H_{TL} from (1)

$$H_{TL} = M_W\ddot{x}_{WL} + H_L \tag{30}$$

Differentiate (4)

$$\ddot{\theta}_{WL} = \frac{\ddot{x}_{WL}}{R} \tag{31}$$

Substitute (30) into (3) than

$$\begin{cases} H_L = \frac{T_L}{R} - \ddot{x}_{WL}\left(M_W + \frac{J_W}{R^2}\right) & \text{for the left wheel} \\ H_R = \frac{T_R}{R} - \ddot{x}_{WR}\left(M_W + \frac{J_W}{R^2}\right) & \text{for the right wheel} \end{cases} \tag{32}$$

Subtract two equation of (32) and then substitute into (18) than

$$\left(J_\delta + \frac{1}{2}D^2\left(M_W + \frac{J_W}{R^2}\right)\right)\ddot{\delta} = \frac{1}{2}D\frac{T_L - T_R}{R} \tag{33}$$

We have

$$J_W = \frac{1}{3} M_B R^2 = J_\delta = \frac{1}{3} M_B \left(\frac{D}{2}\right)^2 = \frac{1}{12} M_B D^2 \tag{34}$$

Substitute (34) into (33) than we get

$$\ddot{\delta} = \frac{6}{(M_B + 9M_W)DR}(T_L - T_R) \tag{35}$$

The basic system of equations are (28), (29) and (35).

Let $x_1 = \theta$, $x_2 = \dot{\theta}$, $x_3 = x$, $x_4 = \dot{x}$, $x_5 = \delta$ and $x_6 = \dot{\delta}$. State equations of the e-scooter is rewritten as

$$\begin{cases} \dot{x}_1 = x_2 \\ \dot{x}_2 = f_1(x_1) + f_2(x_1, x_2) + g_1(x_1)(T_L + T_R) \\ \dot{x}_3 = x_4 \\ \dot{x}_4 = f_3(x_1) + f_4(x_1, x_2) + g_2(x_1)(T_L + T_R) \\ \dot{x}_5 = x_6 \\ \dot{x}_6 = g_3(T_L - T_R) \end{cases} \tag{36}$$

$$f_1(x_1) = \frac{\left(\frac{-0.75g(\sin x_1)}{L}\right)}{\left(\frac{0.75(M_W R + M_B L(\cos x_1))(\cos x_1)}{(2M_W + M_B)L} - 1\right)}$$

$$f_2(x_1, x_2) = \frac{\left(\frac{0.75 M_B L(\sin x_1)(\cos x_1)}{(2M_W + M_B)L}(x_2)^2\right)}{\left(\frac{0.75(M_W R + M_B L(\cos x_1))(\cos x_1)}{(2M_W + M_B)L} - 1\right)}$$

$$g_1(x_1) = \frac{\left(\frac{0.75\left(1 + (\sin x_1)^2\right)}{M_B L^2} + \frac{0.75(\cos x_1)}{(2M_W + M_B)RL}\right)}{\left(\frac{0.75(M_W R + M_B L(\cos x_1))(\cos x_1)}{(2M_W + M_B)L} - 1\right)}$$

$$f_3(x_1) = \frac{\left(\frac{-0.75g(M_W R + M_B L(\cos x_1))(\sin x_1)}{L}\right)}{\left(2M_W + M_B - \frac{0.75(M_W R + M_B L(\cos x_1))(\cos x_1)}{L}\right)}$$

$$f_4(x_1, x_2) = \frac{M_B L(\sin x_1)(x_2)^2}{\left(2M_W + M_B - \frac{0.75(M_W R + M_B L(\cos x_1))(\cos x_1)}{L}\right)}$$

$$g_2(x_1) = \frac{\left(\frac{0.75(M_W R + M_B L(\cos x_1))\left(1 + (\sin x1)^2\right)}{M_B L^2} + \frac{1}{R}\right)}{\left(2M_W + M_B - \frac{0.75(M_W R + M_B L(\cos x_1))(\cos x_1)}{L}\right)}$$

$$g_3 = \frac{6}{(M_B + 9M_W)DR} \text{ where } \begin{cases} U1 = T_L + T_R \\ U2 = T_L - T_R \end{cases}$$

3.2 Dc Motor Modeling

Dc motor is the most common type of actuator in electric drives mainly because of high starting torque and wide range of speed control. The couples system with the Dc motor may change the rotational motion to translational motion [11, 12]. In this research, Dc motor is considered as the main actuator for the specified application. The schematic diagram of the electric and mechanical components of a Dc motor is given in Fig. 5.

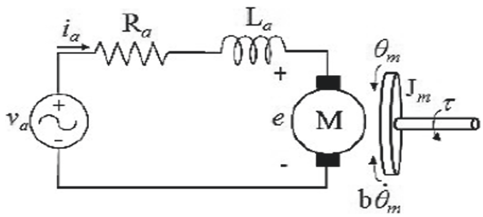

Fig. 5. Schematic diagram of a DC-motor [12]

Applying Kirchhoff's law we can get the electrical equation,

$$v_a = R_a i_a + L_a \frac{d}{dt} i_a + e \tag{37}$$

To drive the mathematical representation of the mechanical part of the motor, the direct proportion relation of the torque with armature current is considered. For the specified application in this research, constant magnetic field is considered and the torque can be affected by the armature current as shown in Eq. (38).

$$T_e = k_t I_a \tag{38}$$

The relation between back emf and angular velocity of the shaft can be represented using Eq. (39).

$$e = k_b \omega \tag{39}$$

Usually, the back emf constant and torque constant are assumed to have same value [11]. Using physical laws, Newton's second law, the expression for the torque can be given by Eq. (40).

$$T_e = J\frac{d\omega}{dt} + B\omega \tag{40}$$

Substitute (39) into (37) and solve I_a of (38) and substitute again into (37) then

$$V_a = \frac{R_a}{K}T_e + \frac{L_a}{K}\frac{dT_e}{dt} + K\omega \tag{41}$$

Now, taking the Laplace transform of (40) and (41)

$$V_a(s) = \frac{R_a}{K}T_e(s) + \frac{L_a}{K}sT_e(s) + K\omega(s) \tag{42}$$

$$T_e(s) = (Js + B)\omega(s) \tag{43}$$

Solve for $\omega(s)$ of (43) and substitute into (42) and solve transfer function of input $V_a(s)$ and output $T_e(s)$ than

$$V_a(s) = \left(\frac{R_a}{K} + \frac{L_a}{K}s + \frac{K}{Js + B}\right)T_e(s)$$

Then

$$T_e(s) = \frac{K(Js + B)}{R_a(Js + B) + L_a s(Js + B) + K^2}V_a(s) \tag{44}$$

From motor dynamics, the torque driving the right and left wheel can be expressed as [12].

$$U_1 = \frac{K(Js + B)}{R_a(Js + B) + L_a s(Js + B) + K^2}(V_L + V_R)$$
$$U_2 = \frac{K(Js + B)}{R_a(Js + B) + L_a s(Js + B) + K^2}(V_L - V_R) \tag{45}$$

System Decoupling: The state-space representation indicates that two wheel scooter is a high coupled nonlinear system. The decoupling the whole system into two separate sub-systems. Similar to the work in [17, 18] the following decoupling transformation is used to convert V_θ and V_δ to the voltages of the left and right wheels V_L *and* V_R. Where as

$$\begin{cases} V_\theta = V_L + V_R \\ V_\delta = V_L - V_R \end{cases} \tag{46}$$

So

$$\begin{cases} V_L = \frac{1}{2}(V_\theta + V_\delta) \\ V_R = \frac{1}{2}(V_\theta - V_\delta) \end{cases} \tag{47}$$

where,

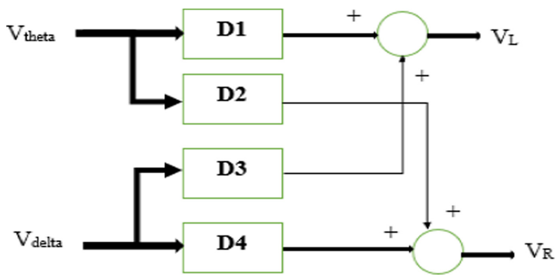

Fig. 6. Decoupling unit

$$D1 = D2 = D3 = 0.5 \text{ and}$$
$$D4 = -0.5$$

The parameter values of the scooter and the dc-motor specifications for the proposed system drive are given Tables 2 and 3 respectively.

Table 2. Parameter of scooter with specified value [1, 8].

symbol	Value (unit)	Description
θ	Degree	Pitch angle (user defined)
δ	Degree	Yaw angle (user defined)
M_W	6kg	Mass of the wheel
M_B	Up to 90kg	Mass of the body
R	0.2m	Radius of the wheel
L	1m	Distance between z-axis and e gravity center
D	0.6m	Distance between contact patches of the wheel
g	9.8m/s^2	Acceleration due to Gravity

Table 3. DC motor value

Parameters	Description	Value (unit)
Ra	Armature Resistance	2.5 Ω
La	Armature Inductance	0.0005H
Va	Armature Voltage	V
e	DC motor Back Emf	V
Kb	DC motor back emf constant	0.58V s/rad
Kt	DC motor torque constant	0.58 N m/A
ω	DC motor rated speed	rad/s
J	Moment inertia of the motor	0.02 kg.m^2/s^2
B	Damping ratio of the mechanical system	0.04 Nms

4 Controller Design

4.1 Design Super Twisted Sliding Mode Controller (STSMC) for Balancing Scooter

Firstly, we design the sliding mode function as,

$$S = c\dot{e} + e \tag{48}$$

where S is sliding surface, e is error and c must satisfy the Hurwitz condition.

Define tracking error for the pitch angle as

$$\begin{cases} e = x_1 - x_{1ref} \\ \dot{e} = \dot{x}_1 - \dot{x}_{1ref} \\ \ddot{e} = \ddot{x}_1 - \ddot{x}_{1ref} = \dot{x}_2 - \ddot{x}_{1ref} \end{cases} \tag{49}$$

where $x_{1ref} = \theta_{ref}$, the reference value of pitch angle.

Therefore, we have

$$\dot{S} = c\dot{e} + \ddot{e} = c(\dot{x}_1 - \dot{x}_{1ref}) + (\dot{x}_2 - \ddot{x}_{1ref})$$

But

$$\dot{x}_2 = f_1(x_1) + f_2(x_1, x_2) + g_1(x_1)U1$$

$$\dot{S} = c(\dot{x}_1 - \dot{x}_{1ref}) + f_1(x_1) + f_2(x_1, x_2) + g_1(x_1)U1 - \ddot{x}_{1ref} \tag{50}$$

$$\dot{S}S = S(c(\dot{x}_1 - \dot{x}_{1ref}) + (f_1(x_1) + f_2(x_1, x_2) + g_1(x_1)U1 - \ddot{x}_{1ref})) \tag{51}$$

In order to make the balancing scooter remains on the surface the Lyapunov stability requirement must be fulfilled i.e. to satisfy the condition $\dot{S}S < 0$, then 1st design conventional sliding mode control as.

$$U1 = \frac{c(\dot{x}_{1ref} - \dot{x}_1) - f_1(x_1) - f_2(x_1, x_2) + \ddot{x}_{1ref} - \eta \text{sgn}(s)}{g_1(x_1)} \tag{52}$$

$$\text{sgn}(s) = \begin{cases} 1, & s > 0 \\ 0, & s = 0 \\ -1, & s < 0 \end{cases}$$

where c and η are constant
From (41) designed controller has two parts.

$$U1 = u_c + u_{eq}$$

So

$$u_c = \eta \text{sgn}(s) \text{ and} \tag{53}$$

$$u_{eq} = \frac{c(\dot{x}_{1ref} - \dot{x}_1) - f_1(x_1) - f_2(x_1, x_2) + \ddot{x}_{1ref}}{g_1(x_1)} \tag{54}$$

The Super-twisting sliding mode controller [13–16] is given by:

$$\begin{cases} u_c = -C_1|s|^{\frac{1}{2}}\text{sgn}(s) + v \\ \dot{v} = -C_2\text{sgn}(s) \end{cases} \tag{55}$$

where c_1 and c_2 are constant
From (48) and (55) we have

$$u = -C_1|s|^{\frac{1}{2}}\text{sgn}(s) - C_2\int_0^t \text{sgn}(s)d\tau \tag{56}$$

Therefore from (54) and (56) the proposed super twisted sliding mode controller is given by

$$U1 = u_c + u_{eq}$$

$$U1 = \frac{c(\dot{x}_{1ref} - \dot{x}_1) - f_1(x_1) - f_2(x_1, x_2) + \ddot{x}_{1ref}}{g_1(x_1)} - C_1|s|^{\frac{1}{2}}\text{sgn}(s) - C_2\int_0^t \text{sgn}(s)d\tau \tag{57}$$

The parameter of STSMC C1, C2 and c are tuned using genetic algorithm (GA). And STSMC are used to control balancing of scooter.

4.2 Design PID Controller for Turn Left and Right Direction

Proportional, integral and derivative controller is also designed to compare the performance of the proposed modern optimization algorithms based tuned controller. The mathematical representation of the PID controller comprising of all actions on the error is given by Eq. (58), defining "u" as the controller output and Kp, Ki and Kd as the corresponding constants [12].

$$U = Kpe(t) + Ki\int e(t)dt + Kd\frac{d}{dt}e(t) \tag{58}$$

4.3 Controller Parameters Tuning Sung GA

The most crucial step in applying GA is to choose the objective functions that are used to evaluate fitness of each chromosome. Some of this objective function are

$$\begin{aligned} IAE &= \int_0^{\tau} |e(t)|dt \\ ISE &= \int_0^{\tau} e(t)^2 \\ ITAE &= \int_0^{\tau} t|e(t)|dt \end{aligned} \tag{59}$$

The STSMC and PID controller is used to minimize the error signals, or we can define more carefully, in the term of error criteria: to minimize the value of performance indices mentioned as below for our system.

$$ITAE = \int_0^{t} t(|e_1(t) + |e_2(t)||)dt \tag{60}$$

where $e_1(t) = \theta_{ref} - \theta(t)$ and $e_2(t) = \delta_{ref} - \delta(t)$

Pseudo code for GA to tune parameter of controller:

1. Generate an initial, random population of individuals for a fixed size
2. Evaluate their fitness.
3. Select the fittest members of the population.
4. Reproduce using a probabilistic method
5. Implement crossover operation on the reproduced chromosomes (choosing probabilistically both the crossover site and the.mates.).
6. Execute mutation operation with low probability.
7. Repeat step 2 until a predefined convergence criterion is met.

The genetic algorithm parameters, the convergence characteristic of the fitness function and tuned parameters are given in Fig. 6. In Fig. 6(b) analytically tuned parameters are also included. From the response the convergence curve, the algorithm converged with best value of 0.0158945, mean value of 0.0162138 and seventh generation (Fig. 7).

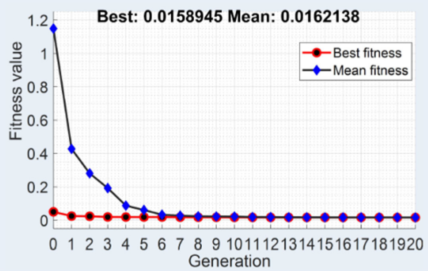

(a) GA convergence curve

GA tuned		Analytical	
Parameter	value	Parameter	value
c	6.3069	c	0.4
C_1	14.0099	C_1	4.72
C_2	10.5369	C_2	14.64
K_d	58.7089	K_d	0.064
K_p	427.7031	K_p	794.58
K_i	273.6920	K_i	3.705
GA-parameters			
Population		40	
Max-generation		20	
Number of parameters		6	

(b) parameter values

Fig. 7. Convergence curve and parameter values

5 Results and Discussions

The simulation is performed based on parameter of scooter described in tables above. STSMC is used for balancing of scooter and PID controller is used for direction control (turn left and turn right). Performance evaluation of the corresponding controllers is done using MATLAB/Simulink.

5.1 GA Tuned Controllers with Initial Pitch and Yaw Angles

Figure 8(a) shows the response of the scooter with small initial pitch angle ($\theta = 0.1$ rad), and the corresponding error plot with reference angle of zero rad. And the response plot for zero reference angle and with initial pitch angle of $\theta = 0.3$ rad is presented in Fig. 8(b).

For both cases of initial pitch angles $\theta = 0.1$ and $\theta = 0.3$, the steady state errors are 7.965×10^{-08} and 9.372×10^{-08} respectively. Which is nearly zero and indicates that for the given reference angle of zero radian, the pitch angle of scooter converge to zero for both initial pitch angle values. It is also indication that the scooter can keep the balance.

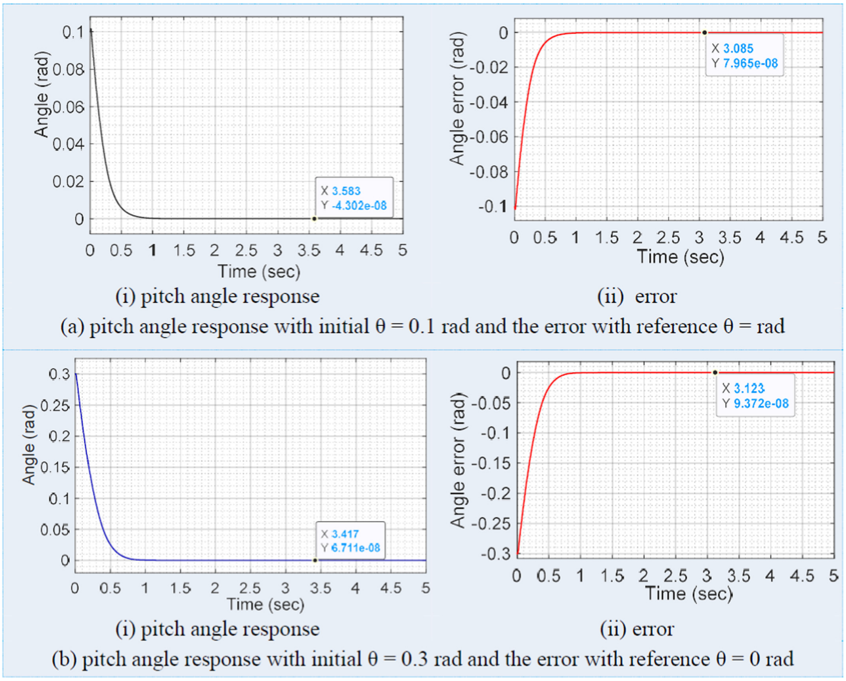

Fig. 8. Pitch angle response with different initial angles and the corresponding error with reference angles

Figure 9 shows the response plot and the corresponding error values of the initial yaw angle, $\delta = 0.1$ rad again for zero reference angel. The direction (turn left and right) of scooter successfully converge to zero.

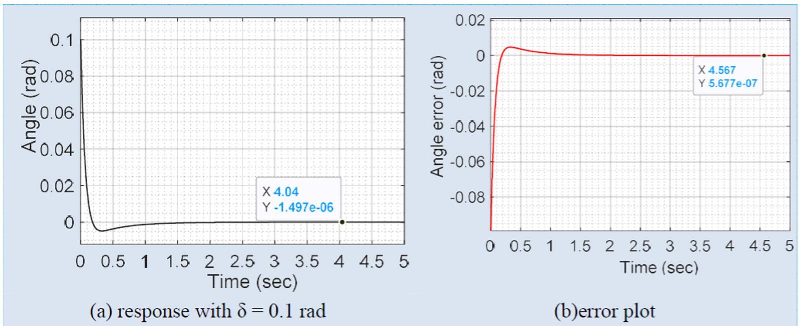

Fig. 9. Yaw angle response with an initial 0.1 rad and the corresponding error from reference angle

5.2 Evaluation of GA and Analytically Tuned Controllers

Comparison of genetic algorithm and analytical method of tuning for STSMC and PID controller for initial pitch angle of 0.3 rad is given in Fig. 10.

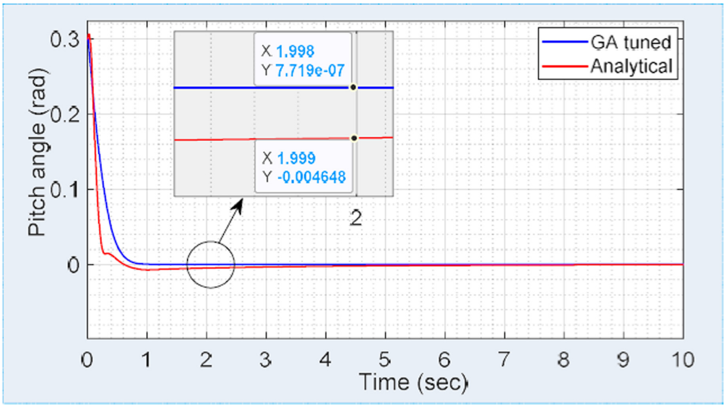

Fig. 10. Pitch angle response with an initial 0.3 rad for Ga tuned and analytical method

The performance evaluation of GA tuned and analytically tuned controllers for the proposed application show that GA tuned parameters gives almost zero steady state error (7.719 × 10–07) compared to analytically tuned controllers (−4.648 × 10–03).

6 Conclusions

Mathematical models of self-balancing scooter, controllers of supper twisted sliding mode add PID design using genetic algorithm and analytical tuning methods has been done. Performance evaluation of controllers tuned in both approaches has been evaluated for initial pitch and yaw angle values of 0.1 and 0.3 rad with zero reference angles has been done. The simulation results show that for both GA tuned and analytically tuned controllers have nearly zero steady state error. However, GA tuned parameters give better convergence to zero and fast dynamic response (settling time) compared with system response with analytically tuned controllers.

References

1. Kamen, D.: Segway (2001). www.segway.com
2. Jmel, I., Dimassi, H., Hadj-Said, S., M'Sahli, F.: Adaptive observer-based Sliding mode control for a two-wheeled self-balancing Robot under terrain inclination and disturbances. Math. Prob. Eng. **2021**, 1–15 (2021)
3. Goher, K.M., Tokhi, M.O., Siddique, N.H.: Dynamic modeling and control of a two wheeled robotic vehicle with a virtual payload. Arpn J. Eng. Appl. Sci. **6**(3), 7–41 (2011)

4. Kim, S., Kwon, S.: Robust transition control of under actuated two-wheeled self-balancing vehicle with semi-online dynamic trajectory planning. Mechatronics **68**, 102366 (2020)
5. Tsai, C.-C., Huang, H.-C., Lin, S.-C.: Adaptive neural network control of a self-balancing two-wheeled scooter. IEEE Trans. Ind. Electr. **57**(4), 1420–1428 (2010)
6. Khaled, M., Mohammed, A., Ibraheem, M.S.: Balancing a two wheeled robot do (July 2009). https://doi.org/10.13140/rg.2.2.25634.63683
7. Rigatos, G., Busawon, K., Pomares, J., Abbaszadeh, M.: Nonlinear optimal control for the wheeled inverted pendulum system. Robotica **38**(1), 29–47 (2019)
8. Son, N.N., Anh, H.P.H.: Adaptive backstepping self-balancing control of a two-wheel electric scooter. Int. J. Adv. Robot. Syst. **11**(10), 165 (2014)
9. Asali, M.O., Hadary, F., Sanjaya, B.W.: Modeling, simulation, and optimal control for two-wheeled self-balancing robot. Int. J. Electr. Comput. Eng. (IJECE) **7**(4), 2008–2017 (2017)
10. Lin, S., Tsai, C.: Development of a self-balancing human transportation vehicle for the teaching of feedback control. IEEE Trans. Educ. **52**(1), 157–168 (2009)
11. Kankhunthod, K., Kongratana, V., Numsomran, A., Tipsuwanporn, V.: Self-balancing robot control using fractional-order PID Controller, 13–15 March 2019, pp 77–82 (2019)
12. Srisertpol, J.: PI controller plus adaptive fuzzy logic compensator for torque controlled system of DC motor, November 2013 (2013)
13. Ouchen, S., Benbouzid, M., Blaabjerg, F., Betka, A., Steinhart, H.: Direct power control of shunt active power filter using space vector modulation based on super twisting sliding mode control. IEEE J. Emerg. Sel. Top. Power Electron. **9**(3), 3243–3253 (2021). https://doi.org/10.1109/JESTPE.2020.3007900
14. Humaidi, A.J., Hasan, A.F.: Particle swarm optimization–based adaptive super-twisting sliding mode control design for 2-degree-of-freedom helicopter. Measur. Control **52**(9–10), 1403–1419 (2019)
15. Zhao, Y., Huang, P., Zhang, F.: Dynamic modeling and super-twisting sliding mode control for tethered space robot. Acta Astronaut. **143**, 310–321 (2018)
16. Zheng, Z., Teng, M.: Modeling and decoupling control for two-wheeled self-balancing robot. In: 2016 28th Chinese Control and Decision Conference (CCDC) (2016)
17. Chen, L., et al.: Robust hierarchical sliding mode control of a two-wheeled self-balancing vehicle using perturbation estimation. Mech. Syst. Sig. Process. **139**, 106584 (2020)
18. Ali, M.I., Hossen, M.M.: A two-wheeled self-balancing robot with dynamics model. In: 2017 4th International Conference on Advances in Electrical Engineering (ICAEE), Dhaka, 2017, pp. 271–275 (2017)